Bull. Mater. Sci., Vol. 28, No. 2, April 2005, pp. 97–102. © Indian Academy of Sciences.

# Growth and characterization of $Hg_{1-x}Cd_xTe$ epitaxial films by isothermal vapour phase epitaxy (ISOVPE)

**MANJU MALHOTRA, MADHUKAR GAUTAM, J K RADHAKRISHNAN, VINOD KAPOOR, SUDEEP VERMA, UPENDRA KUMAR, ANAND KUMAR, GARIMA GUPTA, ANSHU GOYAL and S SITHARAMAN***

Solid State Physics Laboratory, Lucknow Road, Delhi 110 054, India

MS received 20 September 2004; revised 5 February 2005

**Abstract.** **Growth of $Hg_{1-x}Cd_xTe$ epitaxial films by a new technique called asymmetric vapour phase epitaxy (ASVPE) has been carried out on CdTe and CZT substrates. The critical problems faced in normal vapour phase epitaxy technique like poor surface morphology, composition gradient and dislocation multiplication have been successfully solved. The epitaxial films have been electrically characterized by using the Hall effect and capacitance–voltage ($C$–$V$) measurements.**

**Keywords.** **MCT; epitaxy; characterization; vapour phase.**

## 1. Introduction

The ternary II–VI semiconductor, $Hg_{1-x}Cd_xTe$ (MCT), is an important intrinsic alloy material for use as infrared (IR) detector in thermal imaging applications. Its bandgap can be tuned by varying the value of $x$ from 0 to 1 and hence detectors with peak responses in the two atmospheric transmission windows, 3–5 μm and 8–14 μm, can be produced. Further, the outstanding fundamental properties of MCT, e.g. high optical absorption coefficient, high electron mobility, low thermal carrier generation rate and tunable bandgap, make it an excellent material for infrared detectors (Elliot *et al* 1994). During the past 2–3 decades, these alloys have found widespread applications as infrared detectors for military, space and industrial systems.

Several bulk and epitaxial growth techniques have been developed to obtain MCT single crystals. Among the epitaxial techniques, molecular beam epitaxy (MBE), metallo–organic chemical vapour deposition (MOCVD), liquid phase epitaxy (LPE) and isothermal vapour phase epitaxy (ISOVPE) are the most commonly used worldwide. The ISOVPE technique has distinct advantages of producing MCT epitaxial films with good radial compositional uniformity, surface morphology and electrical properties. Moreover, it is a low cost, simple and versatile technique (Adamiec and Miroslaw 1998). Different variations of ISOVPE in open tube (Shin and Pasko 1984; Piotrowski *et al* 1987) and closed tube (Bailly *et al* 1975; Becla *et al* 1982a) configurations have been utilized by different researchers. The major emphasis is on controlling a number of growth parameters viz. temperature, source to substrate distance, time and mercury partial pressure. High capability quasi-closed system have also been used for the growth of device quality epitaxial films of MCT (Piotrowski and Nowak 1988). However, the ISOVPE technique on CZT or CdTe substrates suffers from an inherent disadvantage of composition gradient across the thickness of the film. In this paper, we have tried to overcome the above mentioned critical problems by setting up a new technique called asymmetric vapour phase epitaxy (ASVPE).

## 2. Experimental

Asymmetric vapour phase epitaxy (ASVPE) was carried out under isothermal conditions in a sealed quartz ampoule. There are three main conditions to be fulfilled compared to the experiments conducted in symmetric conditions. The substrate and the ampoule (figure 1) are tilted by 45 degrees which gives rise to parallel line of vapour flow from one end to the other end of substrate. The substrate is placed on the grooves cut in a quartz plug and the top portion of the substrate is covered with a highly polished sapphire plate. The vapours diffuse in the minute gap between the substrate and sapphire plate and hence direct attack of vapours is avoided. The free volume available above the source has to be optimized with respect to the diameter of the quartz ampoule to ensure uniform flux density throughout the substrate area. For example, in our case, quartz ampoule having a diameter of 18 mm and free volume of 65 cc was provided. The substrates used were properly prepared for their surface by mechanical as well as chemo-mechanical polishing in 1% $Br_2$ and $CH_3OH$ solution. The starting material (charge) for the growth of the films was pre-synthesized HgTe prepared from 7 N Hg and $6N^+$

*Author for correspondence (SITHARAMAN/SSPL@ssplnet.org)

Te starting raw materials. The HgTe was powdered and saturated with Te in 9/1 molar ratio to be used as charge for the growth experiments. The substrate was placed at distances varying from 6 to 15 mm above the charge and sealing was done under high vacuum. The experimental arrangement is shown schematically in figure 1. As shown in the figure the substrate to source distance was not same throughout and the free volume above the source was chosen in such a way that the vapour flux available for diffusion in both the distances, $d_{min}$ and $d_{max}$, were the same. Also since the vapours have to pass through the minute gap between the sapphire plate and the substrate for the growth to take place the direct attack of tellurium vapours was minimized resulting in excellent terracing morphology characteristic of LPE grown films. Also the source material was taken in separate bulb at the end of the ampoule which was separated by the rest of the ampoule by a narrow cavity which completely avoids the contact of the source material with the substrate allowing only the vapours to react with the $Cd_{0\cdot96}Zn_{0\cdot04}Te$/CdTe substrate. The growth was carried out keeping the mercury pressure in the system within the existing region of solid HgTe so that the dissociated Te vapours controlled the growth rate.

The growth mechanism is as follows: The deposition takes place in four major steps: (i) dissociative evaporation of the HgTe source, (ii) transport of Hg atoms and $Te_2$ molecules from the source to the substrate, (iii) formation of HgCdTe at the surface of the growing layer and (iv) interdiffusion of components in the layer. The addition of Te allows control of the mercury pressure for growth. The ampoule is heated in a furnace in asymmetric condition where substrate and charge are tilted by 45°. Different

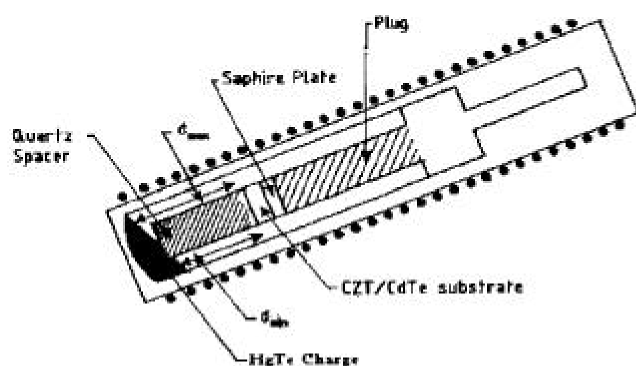


**Figure 1.** Schematic diagram of experimental arrangement for asymmetric vapour phase epitaxy (ASVPE).

substrate temperatures ranging from 470–600°C and growth durations were used. The films were characterized for their surface morphology by optical microscope and SEM. The composition variation along the thickness was measured by EDAX attachment (ISIS 200 EDS System) with SEM. FTIR transmission measurements were done on BIO RAD (FTS-40) for the composition as well as thickness measurement of the films. The crystalline quality of the films was analysed by high resolution rocking curve (DCRC Phillips PW3040/60) X-ray diffraction method using $CuK_{\alpha}$ radiation.

## 3. Control of thickness

In our experiments we have tried to control the thickness by changing the amount of HgTe source taken, time allowed for the diffusion to take place and the temperature of growth. We were able to grow 12–100 μm thick epilayers with sharp interface. Table 1 shows the thickness of the epilayers grown at different temperatures keeping the amount of initial HgTe charge taken and the time of growth, same.

The table below shows that though initial HgTe/Te ratio is approximately same in both the experiments, the higher temperature of growth resulted in higher thickness. The reason being the tellurium diffusion becomes faster at high temperatures which is the key mechanism for the growth of high thickness epitaxial film. The growth rate on CdTe substrates is found to be twice that on $Cd_{0\cdot96}Zn_{0\cdot04}Te$ substrates signifying that the tellurium diffusion coefficient on these two substrates are entirely different and the diffusion rate goes down in $Cd_{0\cdot96}Zn_{0\cdot04}Te$ substrates. Table 2 shows the experimental details of growth on CdTe and CZT substrates.

We have measured the thickness of the epilayers grown on the direct Te vapour exposure side as well as the unexposed side of the substrate from cross-section measurement of the cleaved section in scanning electron microscope and found that thick layers can be grown on the exposed side whereas thin layers can be grown on unexposed side (table 3).

Hence, by controlling various parameters, we are able to control the thickness of the grown epitaxial layers from 12–100 μm. So, for growth of about 30 μm film on the unexposed side of the substrate, a minimum of 20 h growth is necessary for CdTe substrates whereas a minimum of 40 h growth is necessary for $Cd_{0\cdot96}Zn_{0\cdot04}Te$ substrates using

**Table 1.** Variation of thickness of MCT films with growth temperature.

| Sample no. | Amount of charge (g) | Temperature of growth (°C) | Time of growth (h) | Thickness (μm) |
|---|---|---|---|---|
| VPE12 | HgTe 5·7 + Te 0·8 | 590 | 43 | 100 |
| VPE19 | HgTe 4·95 + Te 0·5 | 485 | 43 | 60 |

our experimental set up. The growth rate observed in our experimental set up is of the order of 1·5–2 μm/h on CdTe substrates and about 0·6–1 μm/h on $Cd_{0\cdot96}Zn_{0\cdot04}Te$ substrates which are comparable with the values reported by other workers using ISOVPE (Fleming and Stevanson 1987).

## 4. Composition control

In our work, we have found that the ultimate composition of the MCT epilayer can be controlled by the time of growth after standardizing the partial pressure of Hg and Te inside the free volume between the substrate and the source. This eliminates different Hg partial pressures to be employed for different distances between the source and the substrate (Tufte and Stelzer 1969; Becla *et al* 1982b). Higher time of growth results in lower $x$ values of $Hg_{1-x}Cd_xTe$ since the availability of Cd from the bulk of the substrate for reaction with the HgTe vapours at the surface is depleted as the time progresses. As shown in figure 2, the composition of the epitaxial layers can be tuned by controlling the growth time alone. Lower growth time results in higher surface composition and the subsequent interdiffusion between the bulk and the surface of the epitaxial film during cooling ends to comparatively higher $x$ value. Composition ($x$) of the epitaxial layer was calculated from 50% transmission cutoff wavenumber using the standard formula (Hansen *et al* 1982).

By controlling various parameters e.g. mercury and tellurium partial pressure from the source, substrate temperature, source to substrate distance and time of growth, we were able to control the thickness of the grown epitaxial layers from 12–100 μm with sharp interface. However, the growth rate of ~ 1·5 μm/h was obtained on CdTe substrates whereas growth rate of ~ 0·75 μm/h was obtained on CZT substrates. This is due to the fact that under the same mercury and tellurium partial pressures in the source, the out diffusion of Cd from CZT substrate is reduced due to the presence of Zn.

Various source materials were used e.g. HgTe, HgTe and Te, HgTe and CdTe and surface morphology and composition gradient were studied. Best results were obtained in case of HgTe and CdTe as source material. In this case, growth resulted in 60 micron thick layer with composition gradient of the order of 0·003/μm. As shown in figure 3 the transmission spectrum slope is comparatively sharper and the depth gradient has also been verified by differential chemical etching method. This depth gradient obtained is comparable with LPE grown layers (Norton and Erwin 1989).

**Table 2.** Thickness variation of epitaxial film with time of growth.

| Sample no. | Substrate | Temperature of growth (°C) | Time (h) | Thickness (μm) |
|---|---|---|---|---|
| VPE17 | CZT | 540 | 18 | Few μm |
| VPE18 | CZT | 526 | 45 | 40 |
| VPE28 | CZT | 520 | 45 | 46 |
| VPE14 | CdTe | 510 | 18 | 35 |
| VPE22 | CdTe | 530 | 31 | 55 |
| VPE25 | CdTe | 530 | 16 | 25 |

**Table 3.** Thickness of epitaxial films on two sides of substrate.

| Sample no. | Thickness on exposed side (μm) | Thickness on unexposed side (μm) |
|---|---|---|
| VPE19 | 60 | 12 |
| VPE28 | 46 | 32 |

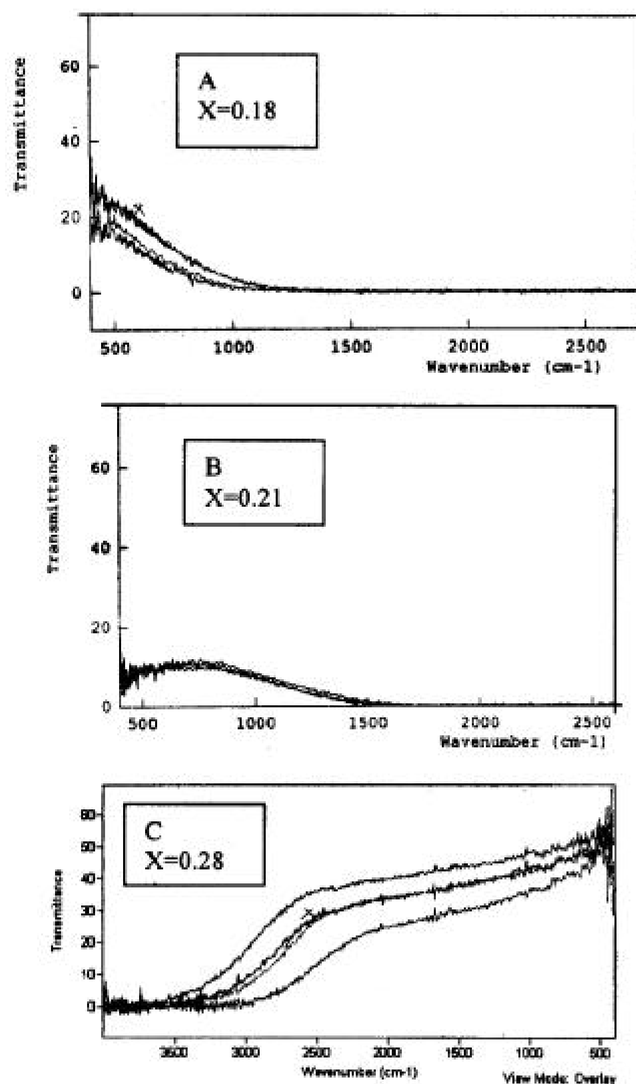


**Figure 2.** FTIR spectra of MCT epilayers grown for (A) 27 h, (B) 21 h and (C) 18 h.

## 5. Surface morphology

The surface morphology of the epilayers were found to be smooth and void-free. The films, in general, showed typical terracing pattern of epitaxial films grown on slightly misoriented substrates ($111 \pm 0{\cdot}5°$) as shown in figure 4. It was observed that irrespective of A or B face of the substrate, the unexposed side resulted in the smoother surface morphology as compared to the exposed side. This is expected to be due to reduced tellurium and cadmium vapour attack on the unexposed side. On the exposed side of the substrate, the tellurium and cadmium vapours are seen to decorate various dislocations of the CZT substrate during the epitaxial layer growth as shown in figure 5.

This effect has been observed by others also (Bagai *et al* 1991), but in our case, we are able to decorate all kinds of defects. Figure 5a shows the decoration of cellular structure whereas figure 5b shows the decoration of grain boundaries. Figures 5c & d show the decoration of micro-precipitates.

## 6. Annealing

In general, as grown films of MCT are *p*-type with carrier concentration of $5 \times 10^{16} - 1 \times 10^{17}$ cm$^{-3}$ and the mobility ~ 150–200 cm$^2$/V-s. Normally, these films are subjected to low temperature annealing in mercury atmosphere in a sealed ampoule to reduce the mercury vacancy concentration (Takigawa *et al* 1988). At the same time, the mercury annealing enhances the defect density in the films due to dislocations being multiplied around the tellurium precipitates (Schaake and Tregilgas 1983). Due to high growth temperature (> 500°C) in VPE process, the tellurium precipitate formation is unavoidable. To overcome this problem, we have utilized the dislocation multiplication reduction (DMR) process (Chandra *et al* 1991) in which high temperature preanneal is carried out before subjecting the films to low temperature anneal. As shown in figure 6a, the as grown layers show IR transmission of ~ 35% which increases to ~ 45% (figure 6b) due to the annihilation of tellurium precipitates, responsible for absorption. In addition to this, the spatial uniformity of the composition is found to be improved on annealing. This can be explained as follows. During the high temperature annealing, the in-diffusing Hg vapours annihilate the tellurium precipitates, forming HgTe complexes which, in turn, further diffuse into the bulk of the film and a rearrangement of composition takes place. Also, it can be observed from figure 7 that CZT/MCT interface is sharp and epilayer is defect-free up to 10 μm (in between two arrows marked) indicating that the accumulated Te precipitates have moved away from the interface to the surface on annealing. The interference fringes obtained in the FTIR transmission spectrum after annealing also reflects the fact that the CZT/MCT interface crystalline quality has improved.

MCT epitaxial layers were non destructively evaluated using high resolution X-ray diffractometer before and after DMR annealing process. As it can be seen from figures 8a and b, the crystalline quality of the MCT epitaxial film has improved after the DMR annealing process as re-

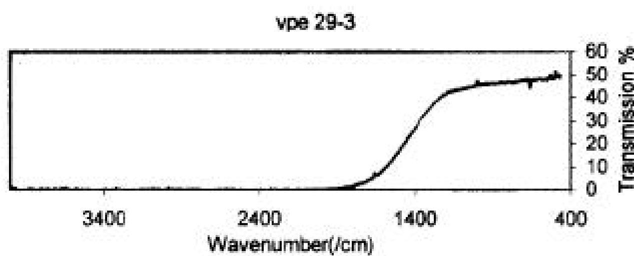


**Figure 3.** FTIR spectrum of $Hg_{0{\cdot}8}Cd_{0{\cdot}2}Te$ epitaxial film using ASVPE technique and source of HgTe and CdTe.

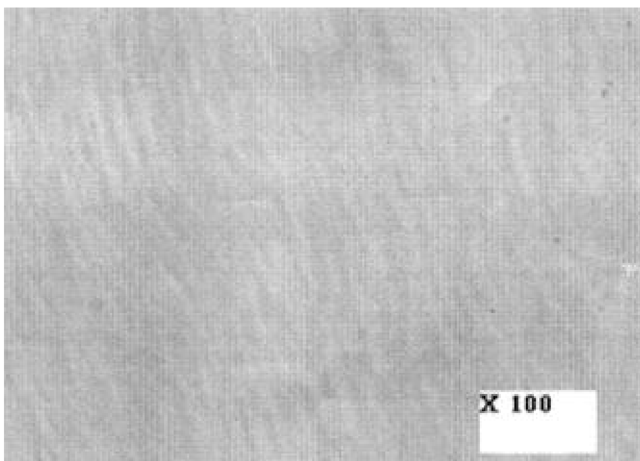


**Figure 4.** Surface morphology of as grown $Hg_{0{\cdot}8}Cd_{0{\cdot}2}Te$ epitaxial film.

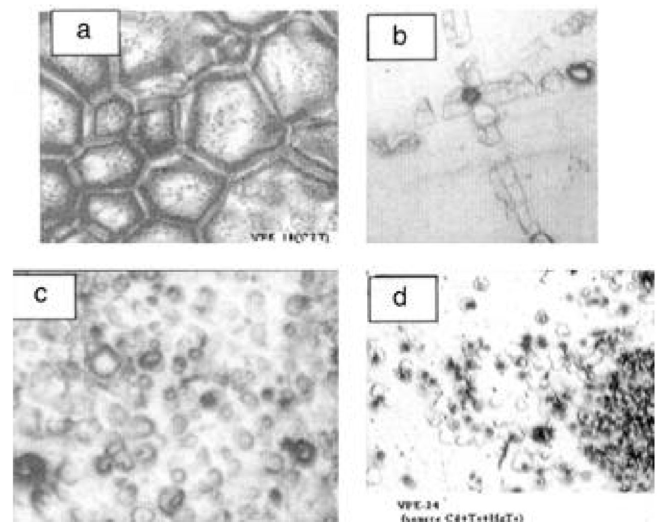


**Figure 5.** Decoration of dislocations during VPE growth by tellurium and cadmium vapours.

flected in the X-ray rocking curve measurements. The double peaks which were predominantly visible in the X-ray rocking curve before annealing have been smoothened after the annealing and the overall FWHM values have reduced considerably from 140 arc s – 80 arc s with large increase in X-ray intensity counts. The corresponding etch pit density (EPD) values as determined by everson etchant have reduced from $10^6/cm^2$ to $10^5/cm^2$ after the DMR annealing process.

These defect density and rocking curve values obtained are comparable with the values obtained in other techniques like LPE, MOCVD (Lu *et al* 1983; Chandra *et al* 1991).

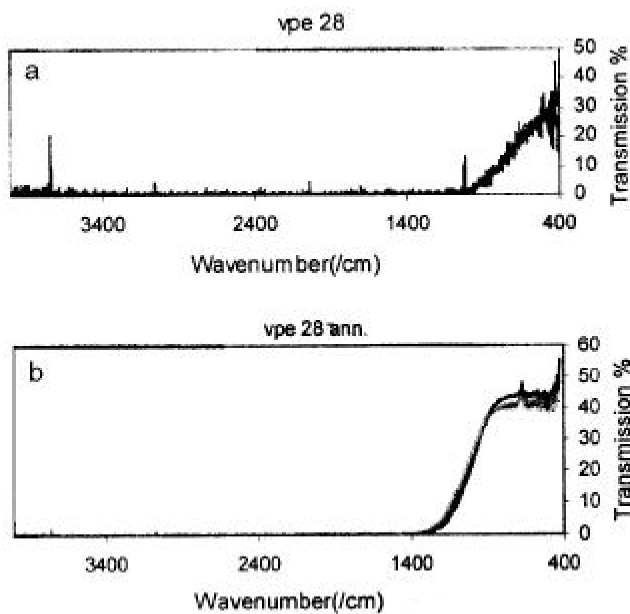


**Figure 6.** **a.** FTIR spectrum of as grown MCT film and **b.** FTIR spectrum of MCT film after the two-step DMR annealing.

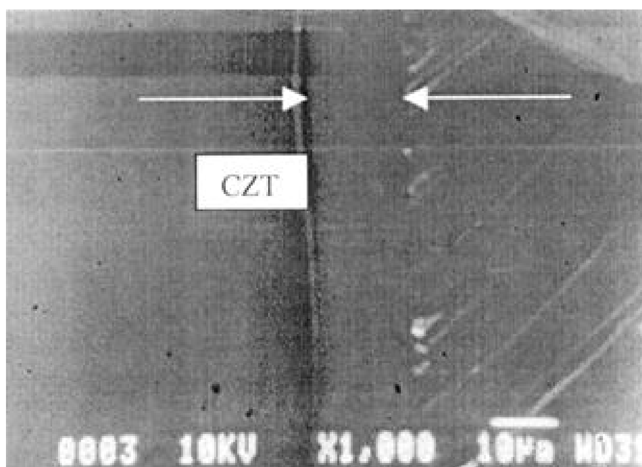


**Figure 7.** SEM picture of CZT/MCT interface after DMR annealing.

## 7. Electrical properties

As grown MCT epilayers were *p*-type with carrier concentration of the order of $1 \times 10^{17}/cm^3$ having mobility of the order of 200 $cm^2$/v-s. These *p*-type layers were subjected to mercury annealing at 200°C for 24 h to convert them to *n*-type films. To understand the compensation mechanism present in the films, variable temperature Hall measurements were carried out on these *n*-type epilayers from room temperature to 10 K (figure 9). The carrier concentration varied from $10^{15}$ to $10^{16}/cm^3$ with temperature and the maximum mobility obtained was $5 \times 10^4$ $cm^2$/v-s. From the logarithmic plot, the activation energy was found to be ~ 0·004291 eV. For most of the II–VI compound semiconductors impurity activation energies are > 0·15 eV (Bube 1960). This low activation energy (4 meV) close to zero obtained in our epitaxial layers suggests that the layer is compensated with intrinsic defects only and do not have any deep level impurity centre for compensation.

Metal insulator semiconductor (MIS) diodes were fabricated on the VPE grown MCT epitaxial films. The surface of the epitaxial layers were chemically prepared using bromine in methanol solution and loaded into the vacuum evaporation chamber for depositing 1000 Å thick ZnS film using photolithographic mask. Au contacts of 50 μm diameter were deposited by thermal evaporation. ZnS film was etched from one corner for enabling the electrical contact to be taken from MCT film. The capacitance–voltage (*C–V*) measurements were carried out using Boonton Capacitance Meter (Model 7200) in the voltage

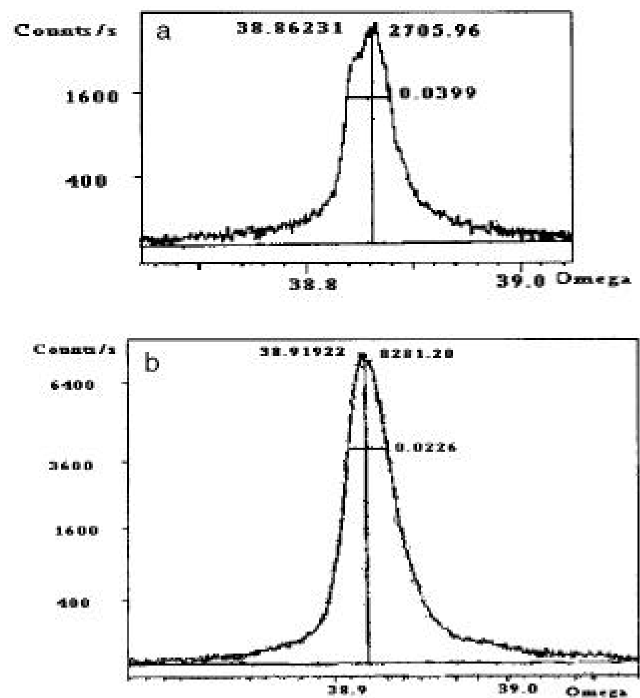


**Figure 8.** X-ray rocking curve **a.** before annealing and **b.** after annealing.

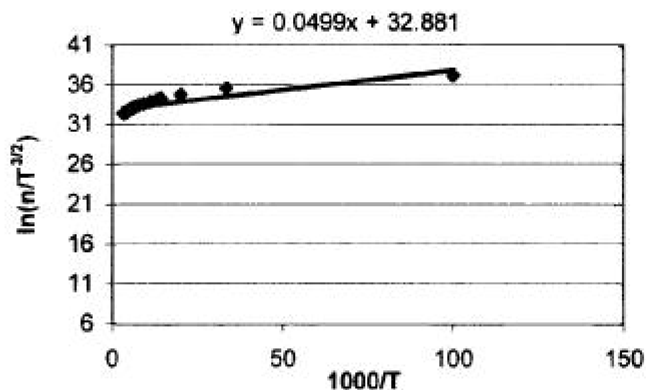


**Figure 9.** Variable temperature Hall measurement on $n$-type MCT film.

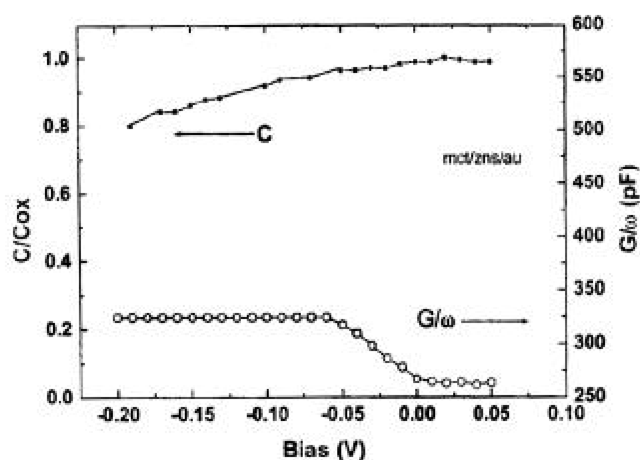


**Figure 10.** Capacitance–voltage ($C$–$V$) and conductance–voltage ($G$–$V$) measurements on MCT film.

range 200–100 mV and 1 MHz frequency. Also the conductance–voltage ($G$–$V$) measurements were carried out. The results are presented for $x = 0{\cdot}2$ $n$-type MCT film in figure 10. As shown in the figure, the conductance curve flattens in the positive voltage range signifying the high frequency performance of the fabricated MIS diodes. The interface states ($Q_f$) were calculated from the $C$–$V$ measurements to be ~ $2 \times 10^{11}$ cm$^{-2}$.

## 8. Conclusions

A new technique called asymmetric vapour phase epitaxy (ASVPE) has been developed to carry out isothermal VPE growth experiments of MCT epitaxial films on CZT/CdTe substrates. This technique solves the problems of non-uniform vapour flux density available at the substrate and the vapour attack on the substrate surface during growth. Dislocation multiplication reduction (DMR) process has been successfully employed to reduce the defect enhancement during the annealing process. Low activation energy values obtained on $n$-type layers suggested that these layers are not compensated by impurities. The MIS diodes fabricated of the grown MCT films showed low interface state density and high frequency performance.

## Acknowledgement

We thank Dr S C Gupta for useful technical discussions.

## References

Adamiec K and Miroslaw G 1998 *Proc. SPIE* **2999** 34
Bailly F, Svob L, Cohen-Solal G and Triboulet R 1975 *J. Appl. Phys.* **46** 4244
Bagai R K, Meenakshi Srivastava, Kailash Sharma and Borle W N 1991 *J. Cryst. Growth* **112** 402
Becla P, Lagowski J, Gatos H G and Jedral L 1982a *J. Electrochem. Soc.* **129** 2855
Becla P, Lagowski J and Gatos H C 1982b *J. Electrochem. Soc.* **129** 1103
Bube R H 1960 in *Photoconductivity of solids* (New York: Wiley)
Chandra D, Tregilgas J H and Goodwin M W 1991 *J. Vac. Sci. Technol.* **B9** 1852
Elliot T 1994 in *Properties of narrow gap cadmium-based compounds* (ed.) P Capper (UK: Inspec. Publ.) p. 1
Fleming J G and Stevanson D A 1987 *J. Crystal Growth* **82** 621
Hansen G L, Schmidt J L and Casselman T N 1982 *J. Appl. Phys.* **53** 7099
Lu P Y, Wang C H, Williams, Chu S N G and Stiles M 1983 *Appl. Phys. Lett.* **49** 1372
Norton P W and Erwin A P 1989 *J. Vac. Sci. Technol.* **A7** 503
Piotrowski J and Nowak Z 1988 *Thin Solid Films* **161** 157
Piotrowski J, Djuric Z, Galus W, Jovic V, Grudzien M, Djinovic Z and Nowak Z 1987 *J. Cryst. Growth* **83** 122
Schaake H F and Tregilgas J H 1983 *J. Electron. Mater.* **12** 931
Shin S H and Pasko J G 1984 *Appl. Phys. Lett.* **44** 423
Takigawa H, Yoshikawa M and Maekawa T 1988 *J. Cryst. Growth* **86** 446
Tufte O N and Stelzer E L 1969 *J. Appl. Phys.* **40** 4559